Internal structure of Einstein-Yang-Mills black holes

E. E. Donets
Laboratory of High Energies, Joint Institute of Nuclear Research, 141980 Dubna, Russia

D. V. Gal'tsov
Department of Theoretical Physics, Moscow State University, 119899 Moscow, Russia

M. Yu. Zotov
Skobeltsyn Institute of Nuclear Physics, Moscow State University, 119899 Moscow, Russia
(Received 31 December 1996; revised manuscript received 18 June 1997)

The interior structure of the static spherically symmetric black holes in the SU(2) Einstein-Yang-Mills theory is investigated both analytically and numerically. It is shown that violation of the no-hair conjecture in this theory has a nontrivial manifestation also inside the event horizon. Although both Schwarzschild and Reissner-Nordström-type interiors still may be realized for certain discrete horizon radii, a generic solution exhibits an infinitely oscillating behavior near the singularity. No inner horizons are formed and the singularity is spacelike, although an infinite sequence of ''almost'' Cauchy horizons is encountered. The amplitude of metric oscillations grows exponentially as the singularity is approached. An approximate two-dimensional dynamical system is derived, which describes an asymptotic structure of space-time near the singularity. [S0556-2821(97)03018-X]

PACS number(s): 04.40.Nr, 04.20.Jb, 04.70.Bw

Discovered soon after the regular Bartnik-McKinnon (BK) solutions [1], Einstein-Yang-Mills (EYM) black holes (see [2–4], and references therein) provided new insight into black hole physics, related to the no-hair and uniqueness issues. It was soon realized that in many non-Abelian field theories the naive no-hair conjecture does not hold and black holes may possess exterior fields that are not generated by the conserved U(1) charges [5]. So far discussion of these solutions has been restricted mostly to the region outside the horizon. Meanwhile, the exterior hair certainly continues inside the black hole and can be expected to cause substantial modification of the interior structure including the singularity.

The nature of a singularity inside a black hole is a fundamental question of the gravitational collapse in spite of the fact that the singularity is hidden from an external observer. It is believed that the space-time outside a compact neutral spherical collapsing body is given by the Schwarzschild solution. An associated singularity is spacelike and strong. However, a small Maxwell field in the case of a charged body changes substantially the nature of the singularity, converting it to timelike. On a perturbative level one observes that, whereas the scalar radiative multipoles generally depending on the Schwarzschild coordinates r, t decay for large t (space coordinate in the interior region) and increase for $r\to 0$ (time coordinate), in the Maxwell case there is a particular spatially homogeneous mode (i.e., depending only on ''time'' r) which diverges as $r\to 0$ and which is responsible for creation of the Cauchy horizon and transformation of the singularity into timelike [6]. Since the Cauchy horizon is unstable [7], this model, however, does not seem realistic, and various attempts were undertaken [8] to understand the nature of a singularity in ''physical'' black holes. Perturbative analysis predicts that generically a strong spacelike singularity should form, perhaps accompanied by the null weak precursor singularity [9].

In non-Abelian gauge theories vector and scalar fields may form non-Coulomb static equilibrium configurations outside the event horizon. Inside the black hole they also constitute homogeneous configurations but essentially different from those in the U(1) case. Since such theories are believed to be more ''generic'' than the Maxwell theory, one can gain new insight into the singularity problem exploring the internal structure of non-Abelian black holes. Our investigation, of which we give brief results here, shows that a generic singularity inside the EYM black holes is strikingly different from those in the Schwarzschild (S) and Reissner-Nordström (RN) solutions. Both S- and RN-type singularities may still be developed but only for a discrete set of the event horizon radii. This ''second quantization'' is similar to the ''first quantization'' of the exterior solutions and mathematically follows from the same kind of nonlinear boundary value problem. Meanwhile a *generic* EYM black hole develops the spacelike singularity of an oscillatory nature. This is conformable with an expectation that no Cauchy horizons should form in ''realistic'' black holes and that the singularity must be of mixmaster type [10]. However, this is not exactly the case since the mixmaster regime corresponds to the Bianchi-type homogeneous three-metric while the interior of a static spherical black hole has as a cosmological counterpart a Kantowski-Sachs spacetime not belonging to the Bianchi family. So the nature of oscillations turns out to be entirely different. Previous qualitative discussion of the EYM black hole interiors can be found in [3].

Assume the static spherically symmetric magnetic ansatz for the YM potential,

$$A=[W(r)-1](T_{\varphi}d\theta-T_{\theta}\sin\theta d\varphi)$$

[$T_{\varphi,\theta}$ are spherical projections of the SU(2) generators], and the following parametrization of the metric:

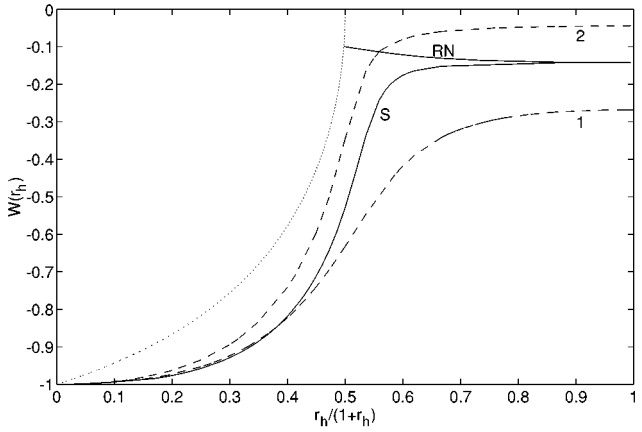

FIG. 1. $W(r_h)$ for the S- and RN-type interior solutions. Dashed lines – $W^n(r_h)$ for $n=1,2$ (higher-n curves lie between the $n=2$ one and the boundary $r_h=1-W_h{}^2$, dotted line). Note that S and RN curves $W(r_h)$ do not merge.

$$ds^2=(\Delta/r^2)\sigma^2dt^2-(r^2/\Delta)dr^2-r^2d\Omega^2, \tag{1}$$

where $d\Omega^2=d\theta^2+\sin^2\theta d\varphi^2$, and Δ, σ depend on r.

The field equations consist of a coupled system for W, Δ,

$$\Delta(W'/r)'+FW'=WV/r, \tag{2}$$

$$(\Delta/r)'+2\Delta(W'/r)^2=F, \tag{3}$$

where $V=(W^2-1)$, $F=1-V^2/r^2$, and a decoupled equation for σ:

$$(\ln\sigma)'=2W'^2/r. \tag{4}$$

These equations admit black hole solutions in the domain $r\geqslant r_h$ for any radius of the event horizon r_h. The solutions are specified by the number $n\in\mathbb{N}$ of nodes of W thus forming a discrete set for each r_h. Although it is not guaranteed *a priori* that the chart (1) is extendible to the full region $r<r_h$, for asymptotically flat solutions one does not meet any singularity in the interior region, unless the genuine one $r=0$ is reached. So the parametrization (1) may also be used under the horizon where $\Delta<0$.

The singular point $r=0$ gives rise to several local solution branches. In terms of coordinates (1) one can find three distinct local power series solutions. The first one is Schwarzschild-like (S); it corresponds to the vacuum value of the YM field $|W(0)|=1$. Using the mass function $m(r)$, $\Delta=r^2-2mr$, one gets [3]

TABLE I. S- and RN-type solutions.

	S-type, $n=1$	RN-type, $n=2$	RN-type, $n=3$
r_h	0.613861419	1.273791	1.0318420
$W(r_h)$	−0.8478649145	−0.113763994	−0.10185163
r_-	—	0.02171654	0.08948446
$W(0)$	−1	−1.212296124	−1.3566052
$\sigma(0)$	0.2263801	5.991210×10^{-3}	1.751928×10^{-3}
Mass	0.8807931	1.018002	1.000277

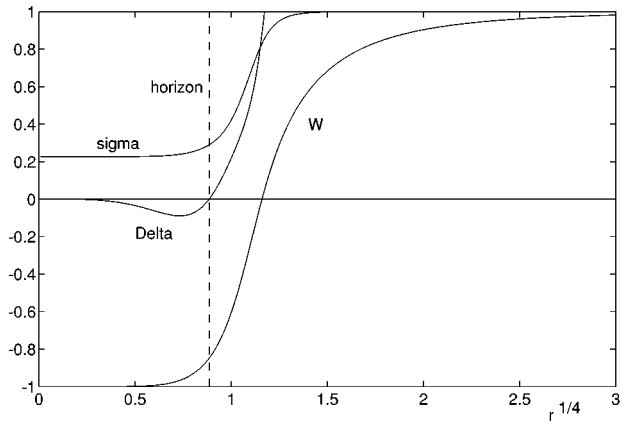

FIG. 2. The $n=1$ EYM black hole (S type).

$$W=-1+br^2+b^2(3-8b)r^5/(30m_0)+O(r^6),$$
$$m=m_0(1-4b^2r^2+8b^4r^4)+2b^2r^3+O(r^5), \tag{5}$$

where m_0, b are (the only) free parameters.

The second is the Reissner-Nordström-type solution, which can be found assuming the leading term of Δ to be a positive constant. This requires $W(0)=W_0\neq\pm1$ and gives [3]

$$W=W_0-W_0r^2/(2V_0)+cr^3/(2V_0)+O(r^4),$$
$$\Delta=V_0^2-2m_0r+r^2+2W_0(c+m_0W_0/V_0^2)r^3+O(r^4), \tag{6}$$

which corresponds to the RN metric of the mass m_0 and the (magnetic) charge $P^2=V_0^2$, $V_0=V(W_0)$. The expansion contains three free parameters W_0, m_0, c.

The third local power series solution can be found assuming a *negative* value for $\Delta(0)$ (i.e., *imaginary* P):

$$W=W_0\pm r-W_0r^2/(2V_0)+O(r^3),$$
$$\Delta=-V_0^2\mp4W_0V_0r+O(r^2), \tag{7}$$
$$\sigma=\sigma_1(r^2\mp4W_0r^3/V_0)+O(r^3).$$

Here there is only one free parameter (W_0) for W, Δ. The corresponding space-time near the singularity is conformal to $\mathbb{R}^2\times S^2$. After a time rescaling one obtains

$$ds^2=r^2(dr^2-dt^2-d\theta^2-\sin^2\theta d\varphi^2). \tag{8}$$

This geometry was encountered in the previous study of black hole interiors in the framework of the perturbed Einstein-Maxwell theory [11,12] and called homogeneous mass inflation (HMI).

It is easy to realize that neither of these asymptotics may correspond to a *generic* black hole. Imposing ''boundary conditions'' in the singularity, we obtain the same kind of singular boundary value problem as one encountered previously in the exterior problem where a similar role is played by the asymptotic flatness condition. The latter is known to result in the ''quantization'' of the allowed values $W^n(r_h)$. The internal ''boundary value'' problem leads to the second ''quantization'' condition, now for the event horizon radius

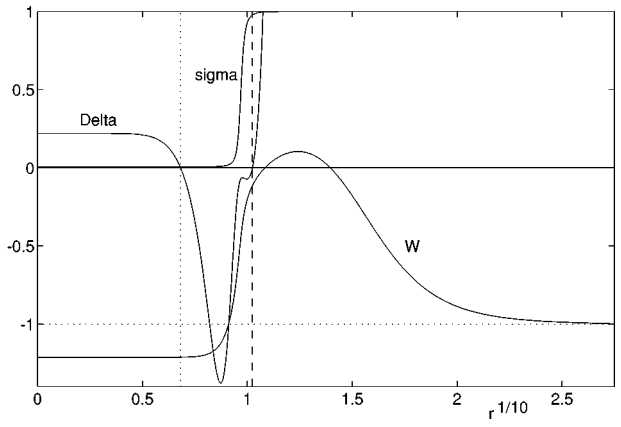

FIG. 3. The $n=2$ EYM black hole (RN type).

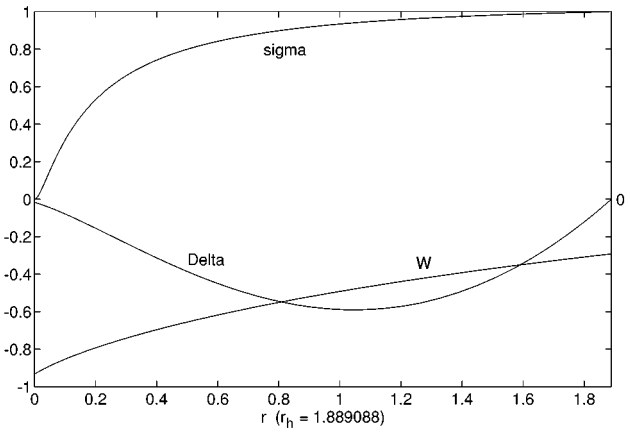

FIG. 5. Interior solution meeting expansions (7) at $r=0$.

r_h. Therefore, EYM black holes with S and RN interiors may constitute only the set of zero measure in the whole EYM black hole solution space. For a generic r_h the interior metric is strikingly different.

The system (2) and (3) was integrated numerically in the region $0<r<r_h$ using an adaptive step size Runge-Kutta method for various $r_h=10^{-8},\ldots,10^{6}$ starting at the left vicinity of the event horizon r_h with one free parameter $W_h=W(r_h)$ satisfying inequalities $|W_h|<1$ and $1-W_h^2<r_h$, which are the necessary conditions for asymptotic flatness (see the Appendix for details). For given r_h, the interior solutions meeting the expansions (5)–(7) may exist only for some appropriate W_h. A numerical strategy used to find such $W(r_h)$ consisted in detecting the change of a sign of the derivative W'. In the S case we found the curve $W(r_h)$, which starts at -1 as $r_h\to 0$ and approaches -0.1424125 for large r_h (Fig. 1) (without loss of generality we choose $W_h<0$). Our S curve intersects the $n=1$ branch of the family of trajectories $W^n(r_h)$, corresponding to the set of external asymptotically flat solutions. Parameters of this black hole solution are shown in Table I, its global behavior is depicted in Fig. 2.

Interior solutions of the RN type, meeting the expansions (6) in the singularity, were found for $r_h>r_h^*=0.990288617$. The corresponding curve $W(r_h)$ (also shown in Fig. 1) intersects the trajectories $W^n(r_h)$ for all $n\geqslant 2$. These solutions possess an inner Cauchy horizon at some $r_-<r_h$ with $|W(r_-)|>1$ (Figs. 3 and 4).

Solutions of the third type (7) were studied numerically, starting from the vicinity of the origin. The unique solution has been found for the horizon data subject to the necessary conditions for asymptotic flatness $|W_h|<1$ and $1-W_h^2<r_h$, for the upper sign in Eq. (7) and $W(0)=-0.9330656$, corresponding to $r_h=1.889088$ (Fig. 5). This solution, however, does not meet any value $W^n(r_h)$ and thus does not represent a black hole. Nevertheless, it is still interesting due to the fact that the metric has no Cauchy horizons. We will come back to this point after discussing the nature of a generic solution.

Hence, we have found that the EYM black holes with the ''standard'' interiors of the S and RN types exist only for certain discrete values of r_h. For all other (continuously varying) r_h one observes oscillations of Δ in the lower half-plane with an infinitely growing amplitude near the singularity. The oscillation region starts with an exponential fall of Δ, which typically occurs after passing a local maximum $r^{\max}$ (Fig. 6). In this regime the right-hand side of Eq. (2) becomes comparatively small with respect to other terms, and one can simplify the system analytically. Neglecting the right side of Eq. (2), one obtains the following (approximate) first integral of the system (2)–(4)

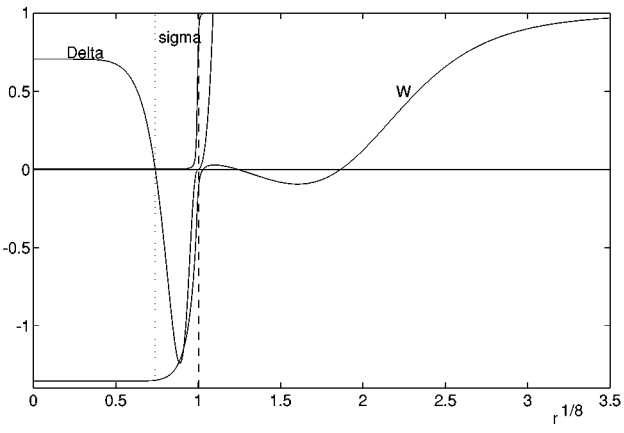

FIG. 4. The $n=3$ EYM black hole (RN type).

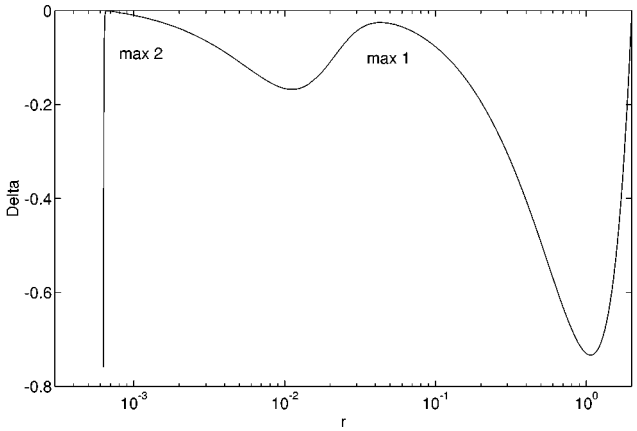

FIG. 6. The beginning of Δ oscillations for $n=1$, $r_h=2$, $W(r_h)=-0.342072$.

TABLE II. Oscillations parameters for $r_h=2$, $W_h=-0.342072$ ($n=1$ black hole).

	r	$W(r)$	$W'(r)/r$	$\Delta(r)$
$r_1^{\max}$	4.32×10^{-2}	-0.881410	27.89	-2.52×10^{-2}
$r_1^{\min}$	1.12×10^{-2}	-0.922056	67.03	-1.68×10^{-1}
$r_2^{\max}$	6.63×10^{-4}	-0.926862	7.30×10^{3}	-4.16×10^{-4}
$r_2^{\min}$	4.73×10^{-5}	-0.930103	1.49×10^{4}	-8.12×10^{36}
$r_3^{\max}$	6.44×10^{-44}	-0.930120	4.10×10^{81}	-1.36×10^{-79}
$r_3^{\min}$	8.81×10^{-83}	-0.930136	8.01×10^{81}	$-2\times10^{1.16\times10^{77}}$
$r_4^{\max}$	$2\times10^{-1.16\times10^{77}}$	-0.930136	$0.5\times10^{2.32\times10^{77}}$	$-2\times10^{-2.32\times10^{77}}$

$$Z=\Delta W'\sigma/r^2=\text{const.} \tag{9}$$

In what follows we will describe in more detail the lower n case (qualitatively the behavior of Δ in the oscillating regime is the same for all n). Starting from some point r_0 close to $r^{\max}$ ($r_0\lesssim r^{\max}$) the quantity $U=W'/r$ becomes approximately constant $U=U_0\gg 1/r^{\max}\gg 1$ ($r^{\max}\ll 1$ for lower n). Then, using Eqs. (3) and (9), one finds the following expression for Δ valid in the region of the exponential fall [13]

$$\Delta(r)=\frac{\Delta(r_0)}{r_0}r\exp[U_0^2(r_0^2-r^2)]. \tag{10}$$

From this expression it is clear that the fall must stop at the local minimum

$$r^{\min}=(\sqrt{2}|U_0|)^{-1}.$$

According to (9) and (10), σ decreases exponentially during the fall of Δ:

$$\sigma^{\min}\sim\sigma^{\max}\exp[-(U_0r^{\max})^2],\quad U_0r^{\max}\gg 1$$

(typically $r^{\min}\ll r^{\max}$). After $r^{\min}$ is passed, U still remains almost unchanged, and hence the exponential factor in Eq. (10) becomes irrelevant. It follows that after passing the minimum, Δ starts to increase linearly so that $|\Delta/r|\approx 2m$ is constant. This regime breaks down when $|\Delta|$ becomes comparable with V^2. Then a rapid growth of U takes place, while σ is still varying slowly. Since the coordinate r practically remains unchanged, from Eq. (9) one can see that the product $U\Delta$ remains almost constant. Finally Δ reaches the next local maximum (asymptotic points of local maxima approaching zero), and then a new oscillation cycle starts with an increasing amplitude (Table II, Figs. 7, 8). It is clear from Eq. (4) that σ monotonically decreases while going leftwards, exhibiting rapid falls during exponential falls of Δ and keeping almost constant values while Δ is increasing. Thus, σ tends to (but does not reach) a zero limit as $r\to 0$.

Although the derivative W' takes rather large absolute values on some intervals, the corresponding variation of W is still small because these intervals are also extremely small. All the above features (small variation of Z and W, constancy of U while $|\Delta|$ is falling down) become more pronounced while oscillations progress, implying that both Z and W have finite limits as $r\to 0$. Then neglecting the right side of Eq. (2), omitting 1 in F, and replacing W by its limiting value W_0, one arrives at the following two-dimensional autonomous dynamical system:

$$\dot q=p,\quad \dot p=(3e^{-q}-1)p+2e^{-2q}-1/2, \tag{11}$$

where $\Delta=-(V_0^2/2)\exp(q)$, and an overdot stands for derivatives with respect to $\tau=2\ln(r_h/r)$. This system has one (focal) fixed point ($p=0$, $q=\ln 2$) with eigenvalues $\lambda=(1\pm i\sqrt{15})/4$; its phase portrait is shown in Fig. 9 together with an invariant set $p=-e^{-q}-1/2$ corresponding to

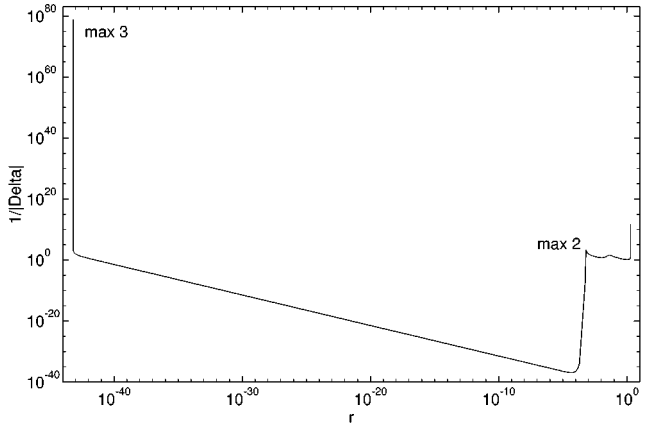

FIG. 7. $|\Delta|^{-1}$ for the second oscillation of $n=1$ black hole solution with $r_h=2$, $W_h=-0.342072$.

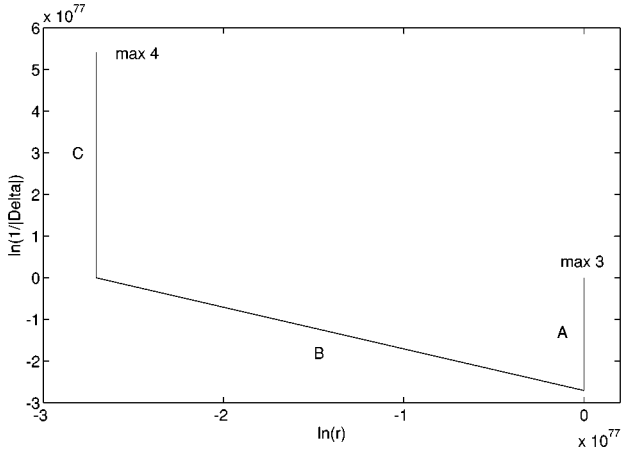

FIG. 8. $\ln(|\Delta|^{-1})$ for the third oscillation.

the RN-type solution. The oscillating solutions lie above this curve. The phase motion in this region is unbounded, and there are no limiting circles. The limit $q=-\infty$ ($\Delta=0$) cannot be reached, Δ remains negative valued as $r\to 0$ and passes an infinite sequence of local maxima and minima (Fig. 9).

Thus, the YM hair in non-Abelian black holes is not only an ''exterior'' phenomenon. It also has important implications on the structure of the singularity hidden inside the event horizon. Remarkably, the nature of the singularity dominated by the YM ''interior hair'' is fairly compatible with general expectations based on the strong cosmic censorship (absence of internal Cauchy horizons) and an oscillatory nature of the generic cosmological singularity [10]. Another (nonoscillating) regime compatible with the strong cosmic censorship could be the RN-type solution with the imaginary charge (7), also known as the HMI solution [12]. But in the present context the HMI internal solution is not asymptotically flat. Deviating from the horizon data that correspond to the interior HMI solution, one is pushed to the continuous set of oscillatory solutions. It has to be noted that the nature of oscillations in our case is essentially different from that in the mixmaster solution. The first reason is that the static spherical black hole interior does not belong to any of the Bianchi types in the cosmological interpretation. The second distinction is that the singularity is matter dominated with a specific form of the YM field configuration.

The solutions obtained are essentially nonperturbative in a sense that the internal hair is not small. It is interesting to note, however, that in the earlier discussion of the black hole interiors both HMI and oscillating regimes were detected in the framework of the perturbed Einstein-Maxwell theory. Namely, as we have already discussed, a model of charged black hole interior with t-independent crossflows of ingoing and outgoing radiation developed in [11] admits a particular solution [12] with the asymptotic Eq. (7). Analyzing an asymptotic form of a more general solution to the same model, Page [11] was able to derive recurrent formulas showing infinite oscillations with growing amplitude. The model is rather different from the present one, although both have important common features such as a conformal nature ($T^{\mu}_{\mu}=0$) and a homogeneity (dependence only on r) of the matter source. Note that our definition of the mass function is different from that in [11,12]: in our case there is no reason to extract the charge contribution from Δ.

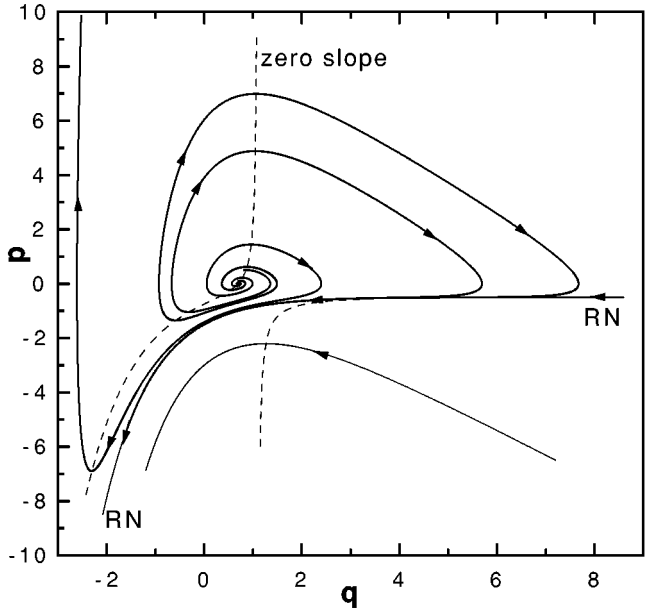

FIG. 9. Phase portrait of (11), RN: an invariant set, corresponding to the RN-type solution (dashed: zero slope lines).

The influence of the black hole ''interior hair'' on the singularity is likely to be a general phenomenon in the non-Abelian field theories. The ''second quantization'' precludes the possibility of the standard S- or RN-type interiors in the generic solutions. A generic regime may be either of oscillatory type, or exhibit a power-law divergence of the mass function near the singularity. Asymptotic solution of this second type, which is realized, e.g., for the Einstein-Yang-Mills-dilaton (EYMD) theory [14], turns out to be generic by counting free parameters. The power index itself is one of such parameters.

The analysis given here is purely classical. A few words are in order about the relevance of the results to the full quantum theory. Vacuum polarization of the conformal scalar field on the HMI background was considered in [12], it was found that the correction to the mass function diverges more strongly than in the classical case. Hence the singularity is not smoothened but rather intensified. In the oscillating regime there is no hope to compute quantum effects quasiclassically. Moreover, huge values of the mass function (in Planck's units) encountered soon after entering such a regime indicate that quantum behavior of the model should be considered nonperturbatively and may well be qualitatively different from the classical picture. However, the conclusion about the spacelike nature of the generic singularity is unlikely to be changed.

Note added. We have become aware of the paper by Breitenlohner, Lavrelashvili, and Maison (gr-qc/9703047), who treated essentially the same subject and tried to generalize the results to the Einstein-Yang-Mills-Higgs (EYMH) theory. Their interpretation of the generic EYMH mass function $m(r)$ as exponentially inflating towards the singularity is incorrect: in this case an analytic solution exists that shows that $m(r)$ has a power-law singularity similar to EYMD theory [14]. In the pure EYM *black hole* case their results agree with ours, in addition they found S solutions for $n>2$. They have also found a hierarchy of the interior S- and RN-type solutions, as well as some additional interior HMI's corresponding to the horizon data not satisfying the necessary condition for asymptotic flatness $1-W_h^2<r_h$. The relevance of these results to the black hole problem, however, remains unclear. As far as the generic (oscillating) EYM black hole interiors are concerned, the qualitative discussion in their paper essentially follows our discussion given earlier, and a dynamical system describing asymptotic behavior near the singularity is the same as our Eq. (11) up to notation. Note that in our numerical calculations we were able to observe more huge oscillation cycles applying the technique of integration along integral curves, see Appendix. We are grateful to these authors for indicating some misprints and a possible numerical error in the original version of our paper.

Afterwards we obtained analytical formulas for the sequence of characteristic values such as m at maxima and minima of Δ, etc. in oscillation cycles [14]. Two papers by Smoller and Wassermann (gr-qc/9703062, gr-qc/9706039) also became available treating mathematical aspects of the problem.

D.V.G. thanks the Theory Division, CERN for hospitality while the first version of the paper was written. Stimulating discussions with G. A. Alekseev, I. Bakas, G. Clément, I. G. Dymnikova, P. S. Letelier, O. I. Mokhov, M. S. Volkov, and technical assistance of R. N. Zhukov are gratefully acknowledged. The research was supported in part by the RFBR Grant Nos. 96-02-18899, 18126.

APPENDIX

Large numbers given in Table II naturally raise questions about the validity of numerical results obtained. Indeed, a direct application of standard techniques is not sufficient here. So we present some details of the numerical procedures, which were used to integrate (2) and (3) in the region of huge oscillations encountered in generic solutions.

One meets two kinds of problems during numerical integration of Eqs. (2) and (3). First, one has to deal with extremely small values of r as $r\to 0$ and of $|\Delta|$ near its local maxima, as well as with very large values of $|U|$ as $r\to 0$, and of $|\Delta|$ near its local minima. The second difficulty is related to the existence of the extremely small intervals of r on which variation of Δ and U is very fast.

The problems of the first kind can be avoided by substitutions like $\ln(1/r)$, $\ln\ln(1/r)$, etc. for r; $\ln(-\Delta)$, $\ln|\ln(-\Delta)|$, etc. for Δ and similarly for other quantities. The second difficulty has been overcome as follows while obtaining numerical data for three sequential oscillations presented in Table II.

Rewrite the system (2), (3) as

$$DW''+FW'=\frac{1}{x}VW, \tag{A1}$$

$$D'+\left(\alpha W'^2-\frac{1}{2x}\right)D=F, \tag{A2}$$

where $x=(r/r_h)^2$, $D=2\Delta/r_h^2$, $\alpha=4/r_h^2$, $V=(W^2-1)/2$, $F=1-\alpha V^2/x$, and $'\equiv d/dx$. Here W' plays the same role as U in (2), (3). Putting it in a first order form, suitable for the Runge-Kutta procedure

$$W'=P,\quad P'=\frac{1}{xD}V(W+\alpha VP)-\frac{P}{D},$$

$$D'=F-\left(\alpha P^2-\frac{1}{2x}\right)D, \tag{A3}$$

one observes that near the local maxima of D a very small absolute value of denominator xD may cause numerical problems. Though unessential for some first maxima (''max 1'' and ''max 2'' in Fig. 6), this really becomes an obstacle for direct integration as oscillations progress. In fact, integrating system (A3) for $r_h=2$, $W_h=-0.342\,072$, one observes that x practically stops near the third local maximum (''max 3'' in Figs. 7 and 8) with $D\approx -10^{-16}$, $W'\approx 10^{18}$ (on a PC with 15 digits after the decimal point). A simple remedy is to desingularize Eq. (A3) by introducing a parameter t as

$$dx=xDdt. \tag{A4}$$

But this method is only local: it opens a way to go through the chosen local maximum, but does not allow one to reach the next minimum of D. A more general technique consists in integration along the integral curve. Let Γ be a smooth curve, defined by

$$x=\phi(t),\quad y=\psi(t),\quad z=\chi(t),\quad t\in[a,b],$$

where ϕ, ψ, $\chi\in C^1[a,b]$, and $\phi'^2+\psi'^2+\chi'^2>0$ in $[a,b]$. Then the length L of Γ is given by

$$L=\int_a^b\sqrt{\phi'^2+\psi'^2+\chi'^2}dt.$$

This formula suggests a choice of an integration parameter instead of x (or r), which allows one to pass the intervals of apparent ''stops'' of x easily. Introduce a parameter l so that $dl=(W'^2+P'^2+D'^2)^{1/2}dx$ [or, for example, $dl=(1+P'^2)^{1/2}dx$ to integrate along P, etc.], and rewrite the system (A3) adding $t=\ln x$ as a new dependent variable. Changing to $G=\ln(-D)$ one is able not only to pass the third local maximum, but also to reach the third local minimum [see Eq. (10) and Fig. 8]. Thus, the system will read

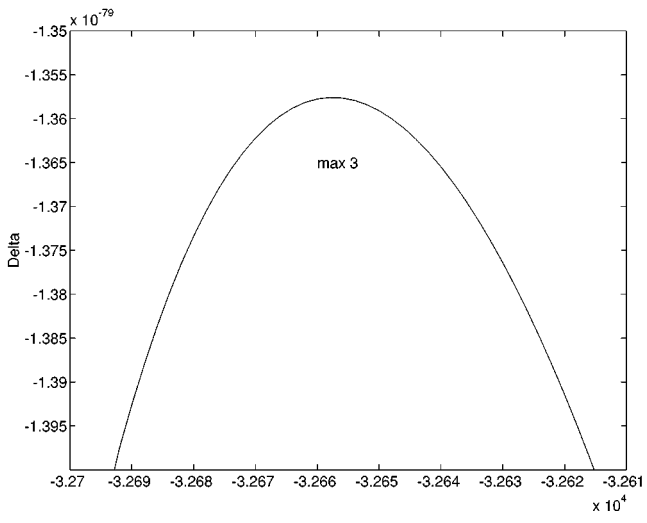

FIG. 10. Δ vs l: the third local maximum.

$$\begin{bmatrix} \dot{t} \\ \dot{W} \\ \dot{P} \\ \dot{G} \end{bmatrix} = \frac{dt}{dl} \begin{bmatrix} 1 \\ e^t P \\ NP - QVW \\ \frac{1}{2} - \alpha e^t P^2 - N \end{bmatrix}, \tag{A5}$$

where $Q=\exp(-G)$, $H=e^t-\alpha V^2$, $N=HQ$, the overdot denotes d/dl, and, e.g., $dl=(1+\dot{G}^2)^{1/2}dt$ for integration along G. This system allows one to go through the third local maximum and along the segments A and B of the third oscillation cycle (Figs. 8 and 10). (Note that B in fact can be passed just using $t=\ln x$ as an independent variable.)

Next, one has to move along the segment C (Fig. 8) and to reach (and pass) the fourth local maximum of Δ. $|\Delta|$ decreases very fast in this interval forcing W' to increase as $|U\Delta|\approx|U(r_3^{\max})|$ [15]. At this step one has to introduce in Eq. (A5) $Z=\ln W'$ [this can be done before passing ''max 3,'' but the original system (A5) works better along the segment A.] Alternatively, one can improve the system in order to integrate along C in a way similar to Eq. (A4). Let us introduce another parameter p, such that $dl=-Ddp$. Then one obtains

$$\begin{bmatrix} \dot{p} \\ \dot{t} \\ \dot{W} \\ \dot{Z} \\ \dot{G} \end{bmatrix} = \frac{dp}{dl} \begin{bmatrix} 1 \\ E \\ E\exp(t+Z) \\ H - VW\exp(-Z) \\ \frac{1}{2}E - H - \alpha E\exp(t+2Z) \end{bmatrix},$$

where $E=\exp(G)$. This system works well both along C and while passing through the local maxima (both ''max 3'' and ''max 4'').

To perform integration in the region of the next oscillation cycle one has to introduce the next order logarithmic substitutions ($\ln\ln(1/x)$, etc.), while the whole numerical strategy remains the same. More details on the subject can be found in gr-qc/9704080. Although an overall accuracy is progressively lost at each step of the calculation, the relative error is kept small.

[1] R. Bartnik and J. McKinnon, Phys. Rev. Lett. **61**, 141 (1988).

[2] M. S. Volkov and D. V. Gal'tsov, Pis'ma Zh. Éksp. Teor. Fiz. **50**, 312 (1989) [JETP Lett. **50**, 345 (1990)]; H. P. Kunzle and A. K. M. Masood-ul-Alam, J. Math. Phys. (N.Y.) **31**, 928 (1990); P. Bizon, Phys. Rev. Lett. **64**, 2844 (1990).

[3] M. S. Volkov and D. V. Gal'tsov, Sov. J. Nucl. Phys. **51**, 747 (1990).

[4] J. Smoller and A. Wasserman, Commun. Math. Phys. **161**, 365 (1994); P. Breitenlohner, P. Forgács, and D. Maison, *ibid.* **163**, 141 (1994); J. Smoller and A. Wasserman, Physica D **93**, 123 (1996).

[5] B. R. Greene, S. D. Mathur, and C. M. O'Neill, Phys. Rev. D **47**, 2242 (1993); P. Bizon, Acta Phys. Pol. B **25**, 877 (1994); T. Torii, K. Maeda, and T. Tachizawa, Phys. Rev. D **51**, 1510 (1995); O. Brodbeck and N. Straumann, J. Math. Phys. (N.Y.) **37**, 1414 (1996); N. E. Mavromatos, Report No. OUTP-96-28P, gr-qc/9606008.

[6] A. G. Doroshkevich and I. D. Novikov, Zh. Éksp. Teor. Fiz. **74**, 3 (1978) [Sov. Phys. JETP **47**, 1 (1978)]; E. Poisson and W. Israel, Class. Quantum Grav. **5**, L201 (1988).

[7] Y. Gursel, V. D. Sandberg, I. D. Novikov, and A. A. Starobinsky, Phys. Rev. D **19**, 413 (1979).

[8] E. Poisson and W. Israel, Phys. Rev. Lett. **63**, 1663 (1989); Phys. Rev. D **41**, 1796 (1990); A. Ori, Phys. Rev. Lett. **67**, 789 (1991); A. Bonnano, S. Droz, W. Israel, and S. M. Morsink, Phys. Rev. D **50**, 7372 (1994).

[9] P. R. Brady and J. D. Smith, Phys. Rev. Lett. **75**, 1256 (1995); A. Ori and E. E. Flanagan, Phys. Rev. D **53**, R1754 (1996); S. Droz, *ibid.* **55**, 4860 (1997); A. Ori, *ibid.* **55**, 3575 (1997).

[10] V. A. Belinskii, I. M. Khalatnikov, and E. M. Lifshitz, Adv. Phys. **19**, 525 (1970); C. W. Misner, Phys. Rev. Lett. **22**, 1071 (1969).

[11] D. N. Page, in *Proceedings of the NATO Advanced Summer Institute on Black Hole Physics*, Erice, 1991, edited by V. De Sabbata (Kluwer, Dordrecht, 1991), p. 185.

[12] W. G. Anderson, P. R. Brady, and R. Camporesi, Class. Quantum Grav. **10**, 497 (1993).

[13] M. Yu. Zotov, M.Sc. of Physics thesis, Moscow State University, 1995.

[14] D. V. Gal'tsov, E. E. Donets, and M. Yu. Zotov, Pis'ma Zh. Eksp. Teor. Fiz. **65**, 855 (1997); D. V. Gal'tsov and E. E. Donets, ''Power-law mass-inflation in Einstein-Yang-Mills-Higgs black holes,'' Report No. DTP-MSU-22/97, gr-qc/9706067.

[15] D. V. Gal'tsov and M. Yu. Zotov, *Teoreticheskie i Eksperimentalnie Problemi Gravitazii*, Tezisi dokladov IX Russkoi Gravitazionnoi Koufezenzii, Moscow, 1996, p. 15.